J Therm Anal Calorim (2015) 120:1355–1364
DOI 10.1007/s10973-014-4300-7

Adsorption and thermal properties of the bovine serum albumin–silicon dioxide system

Małgorzata Wiśniewska · Katarzyna Szewczuk-Karpisz · Dariusz Sternik

Received: 25 September 2014 / Accepted: 9 November 2014 / Published online: 17 December 2014

Abstract The adsorption, electrokinetic, thermal and stability properties of the silicon dioxide (silica, SiO_2)/bovine serum albumin (BSA) system were determined. All measurements were carried out as a function of solution pH value. The highest amount of BSA absorbed on the silica surface was observed at pH 4.6 [the value close to the BSA isoelectric point (pI)], which is primarily related to the packed albumin conformation and the lack of adsorbent–adsorbate electrostatic repulsion. At pH 4.6, largest mass decrease was also noticed (thermogravimetric measurements). At pH 3, 7.6 and 9, the adsorption levels were much lower. This phenomenon is associated with the electrostatic repulsion between the BSA macromolecules and the silica particles as well as the expanded BSA structure. During biopolymer adsorption, the whole solid surface is coated with the albumin macromolecules. Then, the properties of the silica particles become similar to those of the BSA macromolecules. In the presence of albumin, the silica pH_{iep} point is identical to the BSA pI value. It should also be noted that the albumin adsorption affects the SiO_2 suspension stability. The greatest change was observed at pH 3. Under these conditions, the BSA addition causes electrosteric system stabilization.

The present article is based on the lecture presented at ICVMTT 34 conference in Kyiv—Ukraine on 20–21 May, 2014.

M. Wiśniewska (✉) · K. Szewczuk-Karpisz
Department of Radiochemistry and Colloid Chemistry, Maria Curie-Sklodowska University, M. Curie-Sklodowska Sq. 3, 20-031 Lublin, Poland
e-mail: wisniewska@hektor.umcs.lublin.pl

D. Sternik
Department of Physicochemistry of Solid Surface, Faculty of Chemistry, Maria Curie-Sklodowska University, M. Curie-Sklodowska Sq. 3, 20-031 Lublin, Poland

Keywords Silica · BSA · Adsorption · Stability · Zeta potential · Thermal analysis

Introduction

The protein adsorption on the solid surface is a very important process in many scientific areas and industries. In medicine, it is mainly related to implantation. The albumin adsorption on the implant surface is the first process within the body, which occurs shortly after its launch. The course of the above process affects the implant fate, i.e. its acceptance or rejection [1]. Many scientists conducted a study on the protein adsorption on the metal oxide films, because the implants are usually covered with them. Mineral oxide coatings are corrosion resistant and chemically inert [2–5]. In the food industry, the adsorption process can be used for the protein removal from alcoholic beverages, especially beer and wine. Effective removal of these deposits is necessary to maintain the product quality [6, 7]. The protein adsorption on the solid surface also plays an important role in the environmental science. Knowing the process mechanism, an adequate adsorbent can be selected to allow protein removal from water and wastewater [8]. It should be also noted that the described phenomenon is a significant process in the biogeochemical cycles. Binding of proteins, derived from the organic matter decomposition, on the soil particles may result in local poisoning [9]. Thus, given the importance of the protein adsorption, its mechanism as a function of various physicochemical factors should be investigated [10–13]. In the literature, many papers on various properties of amino acids have been also published [14, 15].

In this paper, the adsorption and thermal properties of the bovine serum albumin (BSA)–silica (SiO_2) were examined. The main aim of the study was to examine the BSA adsorption influence on electrokinetic, thermal and stability properties of the silicon dioxide suspension. To accomplish the above object, numerous experimental works, i.e. spectrophotometric, turbidimetric, gravimetric, zeta potential measurements and potentiometric titration, were done. All works were performed as a function of the solution pH value. Protein adsorption on the silica surface is often described in the literature [16, 17]. However, the combination of the biopolymer adsorption with the mineral oxide suspension stability is rare. In addition, reports in the literature on the protein adsorption impact on the colloidal system stability are varied. Wells et al. [18], Allouni et al. [19] and Vamman et al. [20] claimed that the serum protein presence causes the increase of the mineral oxide suspension stability. On the other hand, Flynn et al. [21] observed that the protein addition is associated with the system stability reduction. The work undertaken allowed to see what dependency is found in the BSA–SiO_2 system. It should be also noted that the stability measurement using a turbidimeter is a highly innovative element of the study. This equipment provides very accurate results in the form of TSI (Turbiscan Stability Index) values. Thermogravimetric measurements described in this paper were also made by other researchers [22–26].

BSA is a globular protein, commonly used in biochemistry and molecular biology. BSA is used as an enzyme stabilizer, the protein for the calibration curve preparation, the protein blocking unoccupied binding sites on the nitrocellulose (Western blot, ELISA), a nutrient in cell culture etc. [27]. In turn, silica is a crystalline solid of high hardness, commonly occurring in the earth's crust as quartz. Pure silica is used for the manufacture of quartz glass and silicagel, which is a drying agent and the stationary phase in chromatography. In contrast, silica in the form of sand is used in the manufacture of cement, ceramics, water glass etc. [28, 29]. The choice of the adsorbate and the adsorbent for the experimental work was motivated by their extensive use in research and industry.

Materials and methods

Materials

The fumed silicon dioxide (SiO_2), delivered by *Sigma-Aldrich* company, was used in the experiments. The specific surface area of the adsorbent, determined by the nitrogen adsorption–desorption method, was about 262 $m^2\ g^{-1}$. Based on the Barret, Joyner and Halenda (BJH) method, it was found that there are no micropores in the SiO_2 sample. The average silica particle size, measured using a zetameter, was equal to 225 nm (Fig. 1).

Bovine serum albumin (BSA, *Sigma-Aldrich*) was used as an adsorbate. This is a globular protein of 66 kDa [30]. According to the literature [31, 32], the isoelectric point (pI) of BSA is in the range of 4.7–5. Other scientists calculated that the above point of BSA is equal to 5.56 [33]. BSA is classified as 'soft' protein, i.e. of low internal stability [34]. It was found that at neutral pH, α-helix accounts for 54 % and β-sheet represents about 16–18 % of the BSA chain [35]. Then it is of heart shape [36].

Methods

All measurements were performed at 25 °C using 0.01 M NaCl as a supporting electrolyte. The adsorption, stability, electrokinetic and thermal measurements were carried out as a function of solution pH value (3, 4.6, 7.6 or 9).

Potentiometric titration

The potentiometric titration allowed the determination of sign and density of the SiO_2 surface charge. It was conducted using the computer program 'titr_v3' developed by W. Janusz, and the apparatus consists of Teflon thermostated vessel, water thermostat RE 204 (*Lauda*), glass and calomel electrode (*Beckman Instruments*), pHmeter PHM

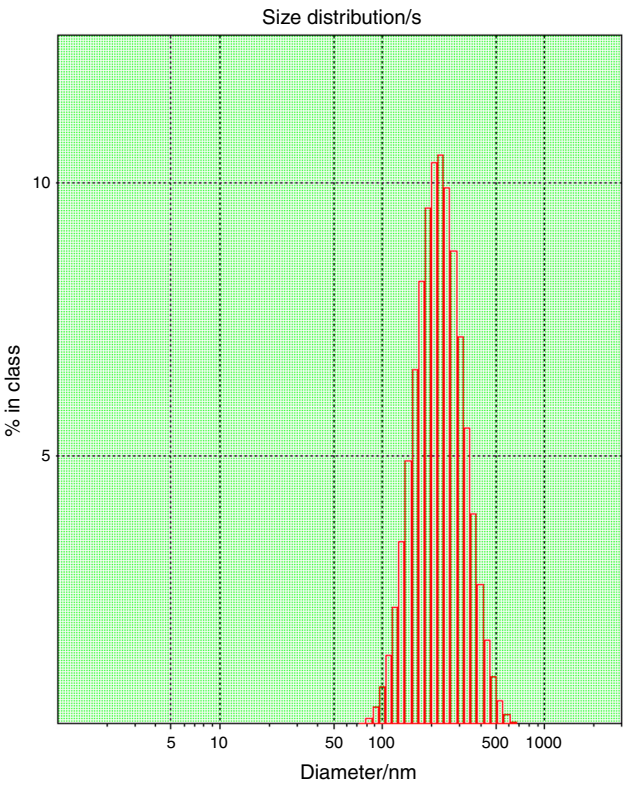

Fig. 1 Silica particle size distribution

240 (*Radiometer*), automatic microburette Dosimat 765 (*Metrohm*), PC and printer. In this method, the surface charge density (σ^0) is determined based on the difference in base volume added to a suspension containing a polymer and a supporting electrolyte solution in order to achieve a specific pH value, using the formula [37]:

$$\sigma^0 = \frac{\Delta V \cdot c \cdot F}{m \cdot S_w}, \quad (1)$$

where ΔV—the difference in base volume added to a suspension and a supporting electrolyte solution that leads to specific pH value ($\Delta V = V_s - V_e$), c—the base concentration, F—the Faraday constant, m—the metal oxide mass in a suspension, S_w—the metal oxide surface area.

At first, potentiometric titration of the supporting electrolyte solution was carried out. Then the SiO_2–NaCl and SiO_2–BSA systems were titrated. The BSA concentration was equal to 10, 50 or 100 ppm. The thermostated vessel was filled with 50 cm^3 of the solution and then 0.1 g of the adsorbent was added. The suspensions were titrated with 0.1 M NaOH. The measurement started at the pH value of approximately 3.5.

Electrokinetic potential measurements

The experiments were carried out using a zetameter Zetasizer Nano-ZS (*Malvern Instruments*). The apparatus was equipped with a titrator which allows automatic solution pH determination during the measurement. Initially, the electrokinetic potential of SiO_2 particles without BSA was measured. Then the systems containing albumin (10, 50 or 100 ppm) were examined. The suspensions were prepared by adding 0.01 g of the adsorbent to the appropriate solution. Each sample was sonicated for 3 min before the measurement.

Adsorption amount measurements

The adsorption level was determined on the basis of the BSA concentration difference in the solution before and after the adsorption process. The BSA concentration was appointed spectrophotometrically (spectrophotometer UV–Vis *Cary 100*, *Agilent Technology*) at 279 nm.

Samples were prepared by adding 0.0085 g of the adsorbent to the appropriately prepared solutions of BSA with the following concentrations: 50, 100, 150, 200, 300, 400 and 500 ppm. The adsorption process was conducted for 1 h. The above time was determined based on the kinetic measurements. After completion of the adsorption process, the samples were centrifuged twice (4,000 rpm), and the obtained supernatants were collected for quantification. A single result of the BSA adsorption amount was the average of three repetitions. The measurement error did not exceed 5 %.

Stability measurements

The stability measurements were performed using a turbidimeter *Turbiscan Lab*^{Expert} with a cooling module *TLab Cooling*. The results were obtained in the form of the curves of transmission and backscatter of light passing through the sample during the measurement. What is more, using the computer software working with the apparatus, the Turbiscan Stability Index (TSI) values were calculated from the following equation:

$$\mathrm{TSI} = \sqrt{\frac{\sum_{i=1}^{n}(x_i - x_{BS})^2}{n-1}}, \quad (2)$$

where x_i—the average backscatter for each minute of measurement, x_{BS}—the average x_i value, n—the scans number.

The stability of the silica suspension in the absence and presence of BSA was measured. The samples were prepared by adding 0.02 g of silica to 20 cm^3 of the appropriate solution (supporting electrolyte or 100 ppm BSA solution). Each suspension was sonicated for 3 min. The albumin was added just before the measurement start. The single measurement lasted 3 h during which the relevant data were recorded every 5 min.

Thermal measurements

The silica and silica–BSA systems were analysed thermogravimetrically using a derivathograph Q-1500D (*MOM Hungary)* [38]. The results were obtained in the form of the following curves: TG (thermogravimetric curve), DTG (differential thermogravimetric analysis curve) and DTA (differential thermal analysis curve). The samples were prepared by adding 0.11 g of silica to the supporting electrolyte or BSA solution (C_{BSA} = 1,300 ppm). After pH value adjustment, the suspensions were shaken for 1 h. In the next step, the precipitate was centrifuged and dried at room temperature. Then the samples were transferred to a measuring chamber which was heated in the range of 20–1,000 °C at a rate of 10 °C per minute.

Results and discussion

The structure of the electrical double layer formed around silica particles in the absence and presence of BSA

The structure of the electrical double layer formed around the silica particles in the absence and presence of BSA was characterized by determining the surface charge density and the zeta potential values of the solid.

Based on the results of the potentiometric titration (Fig. 2), it was found that the pH_{pzc} (point of zero charge) of the silica surface is about 3.1. This means that in a solution of pH equal to this point, the amount of positive (SiO_2^+) and negative (SiO^-) groups on the adsorbent surface is identical. At pH above 3.1, the solid surface is negatively charged. The presence of BSA shifts the pH_{pzc} value to 7.5 (regardless of the albumin concentration). Furthermore, the interaction of BSA with the silica surface causes a slight increase in the solid surface charge. According to Hartvig [39], the effect of the protein adsorption on the adsorbent surface charge density can be calculated using the following equations:

$$\sigma_{ads} = zF\Gamma_{max}\Theta, \tag{3}$$

$$pH_s = pH_{bulk} + 0.434\frac{F\varphi_s}{RT}, \tag{4}$$

$$z_{Ads} = \sum_i^k \frac{10^{pKa_i}}{10^{pH_s} + 10^{pKa_i}} - \sum_j^l \frac{10^{pH_s}}{10^{pH_s} + 10^{pKa_j}}, \tag{5}$$

$$z = \left(\sum_i^m \frac{10^{pKa_j}}{10^{pH} + 10^{pKa_i}} - \sum_j^n \frac{10^{pH}}{10^{pH} + 10^{pKa_j}}\right) + z_{Ads}, \tag{6}$$

where σ_{ads}—the contribution of adsorption to charge density, z—the charge of adsorbed protein macromolecule, F—the Faraday constant, Γ_{max}—the maximum coverage of the surface by the adsorbate, θ—the fractional coverage, pH_s—pH at the surface, φ_s—the potential at the surface, pKa_i—the pKa value of the N-terminus and the side chains of arginine, histidine and lysine of the adsorbed amino acids, pKa_j—the pKa value of the C-terminus and aspartate, glutamate, cysteine and tyrosine amino acid side chains, z_{Ads}—the charge of the interfacial groups.

Thus, the change in the surface charge density as a result of protein adsorption depends on the amino acid sequence and especially on the type of amino acids that are closest to the charged solid surface during adsorption. A slight increase in the silica surface charge in the presence of BSA

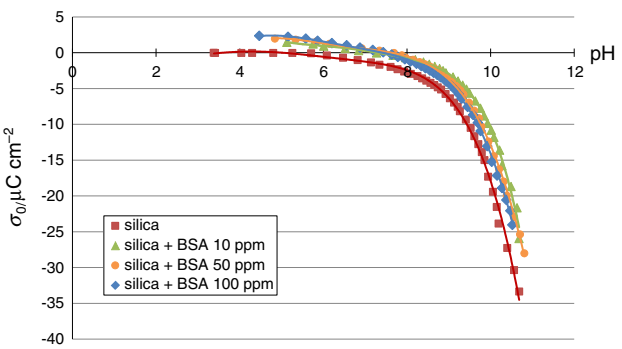

Fig. 2 Sign and density of the silica surface charge in the absence and presence of BSA

can be related to the adsorption of positively charged macromolecules on the negatively charged solid surface. The potentiometric titration started from pH approximately equal to 3.5. Under these conditions, the BSA macromolecules are positively charged due to protonation of the amino groups present in the peptide chain. At higher pH values, the surface charge increase is probably due to the specific macromolecule orientation relative to the solid.

Electrokinetic potential measurements showed that the pH_{iep} of the silica particles is approximately 3.2 (Fig. 3). It means that in a solution of pH 3.2, the concentrations of positively and negatively charged groups in the slipping plane are equal. At pH above this value, the negative groups dominate in the slipping plane, whereas at lower pH the positive ones dominate. The BSA addition moves the pH_{iep} towards less acidic values. The addition of 10 ppm BSA makes the silica pH_{iep} equal to 5.3, whereas the 50 or 100 ppm BSA added makes this point equal to 5.6. The above values correspond to the pl value of BSA. This means that in the BSA concentration range of 10–100 ppm, the silica particle surface is completely covered with the albumin macromolecules. Under these conditions, the adsorbate masks the adsorbent charge and the silica surface exhibits the properties typical of BSA. The described phenomenon was also observed in the electrokinetic study of the chromium(III) oxide suspension in the presence of BSA, HSA and OVA [40] and during the development of a new model for the BSA adsorption on the alumina surface based on the zeta potential and UV–Vis measurements [33].

The BSA adsorption on the silica surface changes the electrokinetic potential values of the solid. In the whole pH range, in the albumin presence, the increase of zeta potential was observed. This is primarily related to the BSA macromolecule charge. In the solutions of pH below the pI value, proteins assume a positive charge due to proton attachment to amino groups. During albumin adsorption, a certain number of positive groups interact with the adsorbent, whereas the remaining part is in the slipping plane contributing to an increase in the zeta potential. In the solutions of pH above the pI value, the protein macromolecules adopt a negative charge, which is mainly due to the proton dissociation from the carboxylic groups. The reduction of the silica electrokinetic potential after BSA addition is the result of the presence of negatively charged functional groups coming from the albumin macromolecules on the slipping plane. Figure 4 shows the most probable structure of BSA adsorption layer at pH 3 and 7.6.

The mechanism of BSA adsorption on the silica surface

The adsorption amount of BSA on the silica surface varies depending on the solution pH value (Fig. 5). The highest

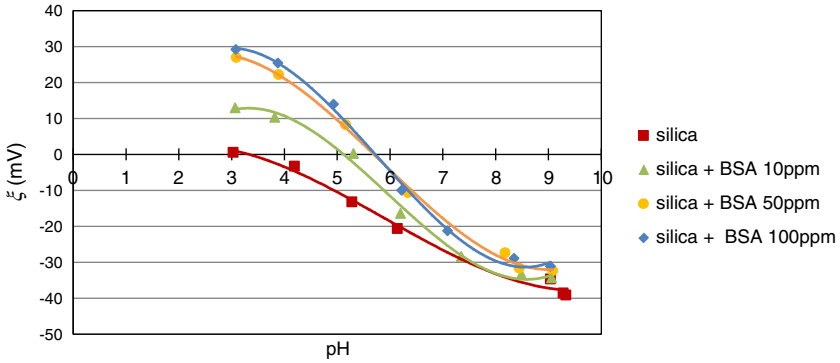

Fig. 3 Electrokinetic potential of the silica particles in the absence and presence of BSA

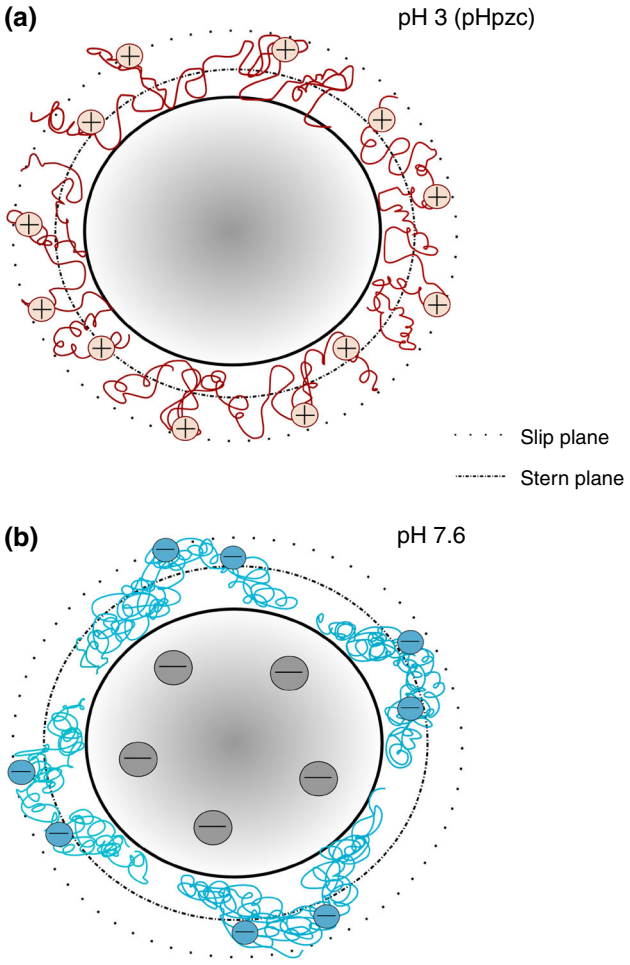

Fig. 4 Structure of BSA adsorption layer at pH 3 (**a**) and pH 7.6 (**b**)

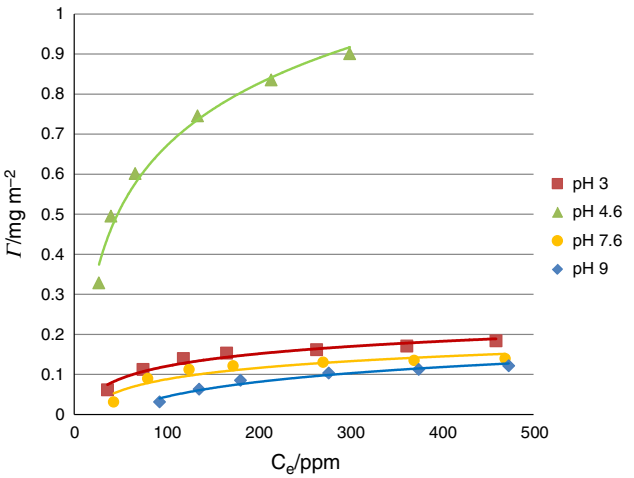

Fig. 5 Adsorption isotherms of BSA on the silica surface at various pH values ($C_{NaCl} = 0.01$ M, $t_{ads} = 1$ h)

amount of the albumin macromolecules gets adsorbed at pH 4.6, i.e. in the solution of pH close to the BSA pI value. Under these conditions, the net charge of the macromolecules is approximately zero—the number of their positive and negative groups is the same. The mutual electrostatic attraction between these groups results in closely packed macromolecule conformation, which results in the high adsorption level on the silica surface. At pH 4.6, the BSA hydrodynamic radius (r_h) is 3.32 nm [30], and the content of α-helix is equal to 55 % [42]. The highly compact structure of the adsorbate allows the adsorption of its maximum amount on the solid surface and formation of highly packed film.

At pH 3, 7.6 and 9, the adsorption amount was significantly smaller compared to that at pH 4.6. This is related to the electrostatic interactions between the solid surface and the albumin macromolecules. Moreover, some domains in the BSA structure are developed, which contributes to the less packed conformation. At pH 3, the adsorption size is higher than at pH 7.6 and 9. Under these conditions, the BSA hydrodynamic radius is 4.31 nm [41] and the content of α-helix is 35 % [42]. The macromolecules of such extended conformation strongly block the access to the adsorbent surface for other macromolecules, which strongly reduces the adsorption amount. At pH 3, the influence of electrostatic forces on the amount of albumin adsorbed is not observed because under these conditions, the adsorbent surface charge is close to 0 ($pH_{pzc} = 3.1$).

At pH 7.6, the BSA adsorption amount is greater than at pH 9. Both at pH 7.6 and pH 9, the electrostatic repulsion

between the adsorbent and adsorbate occurs, which substantially impedes their mutual contact. Under these conditions, the silica particles are negatively charged and the SiO^- groups dominate the surface. The BSA macromolecules are also negative mainly due to the dissociation of carboxylic groups. The albumin adsorption on the silica surface in terms of electrostatic repulsion is equivalent to the presence of hydrogen bond in the system. These bonds are formed in the whole examined pH range. Higher adsorption level at pH 7.6 compared to pH 9 is a result of different BSA conformation. At pH 7.6, the hydrodynamic radius of the macromolecules is 3.57 nm, whereas at pH 9 it is equal to 4.1 nm [41]. Thus, at pH 9, a single macromolecule occupies a larger part of the solid surface than at pH 7.6, which is reflected in lower adsorption amount.

The influence of the BSA adsorption films on the thermal properties of silica

The gravimetric measurements provide significant information which supplements the characteristics of the BSA adsorption mechanism on the silica particles. The results were obtained in the form of curves: thermogravimetric curve (TG), differential thermogravimetric analysis curve (DTG) and differential thermal analysis curve (DTA). The TG curve shows the mass change during heating of the substance as a function of temperature. The DTG curve is calculated as a derivative of the TG curve as a function of time. The analysis of the above curve allows the determination of the initial and final temperatures for each process or reaction. The minimum on this curve shows the temperature of the highest speed of the analysed process. The DTA curve indicates the thermal behaviour of the examined substance during the physical and chemical changes as a function of time. It is plotted based on the temperature difference between the examined substance and the reference one (corundum in this experiment) which does not undergo any physical and chemical changes during measurement. The exothermic reaction is visible on the DTA curve as a curved-up peak, whereas the endothermic reaction—as a curved-down peak.

The obtained results for silica–NaCl and silica–NaCl–BSA at pH 4.6 are shown in Fig. 6 and are summarized in Table 1. Based on their analysis, it was found that the heating process in the range of 20–900 °C of the silica samples without BSA results in two stages (Fig. 6a). The first one, i.e. 20–200 °C is associated with desorption of water which is hygroscopically and physically adsorbed on the silica surface. The above process is endothermic (minimum at 86 °C on the DTG curve). The second stage, i.e. 200–900 °C is associated with the desorption of structural water resulting from silanol condensation of –OH surface groups. The obtained results correspond with the data published by Zaharescu et al. [43].

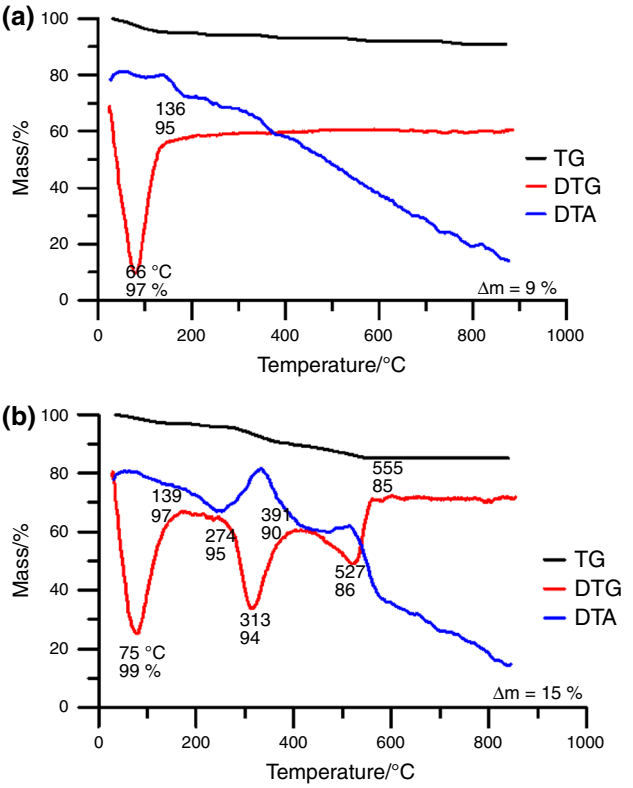

Fig. 6 Thermogravimetric curves for systems: **a** silica, **b** silica–BSA at pH 4.6

As a result of BSA adsorption, the thermal stability of silica changed (Fig. 6b) and the temperatures of different stages shifted to lower values. There are two additional peaks on the DTG and DTA curves in the range 200–600 °C corresponding with the exothermic breakdown of BSA molecules [44, 45]. Due to protein adsorption, its structure is partially denatured and this structure is identical to the thermally denatured form [46, 47]. The first peak in the range of 300–321 °C on the DTA curve is associated with the removal of weakly bound BSA molecules from the surface of the adsorbent (van der Waals forces) and the second one in the range of 457–527 °C—with the decomposition of protein molecules strongly associated with the surface (electrostatic interactions) [48].

The highest mass difference between the samples of silica–NaCl and silica–NaCl–BSA was observed at pH 4.6 (6 %). It is associated with the maximum adsorption of BSA on the silica surface. At pH 3, 7.6 and 9, the mass differences were lower and equal to 3–4 %.

The influence of BSA adsorption on the silica suspension stability

The results of the stability measurements were obtained in the form of curves of light transmission and backscatter. The high transmission and low backscatter indicate a low

Table 1 Thermal decomposition characteristics of silica in the absence and presence of BSA as a function of solution pH value

System	DTG peak positions/°C	Main reaction type: Exo↑/Endo↓	Mass loss/%/in the temperature range:			Total mass loss/%
			20–200/°C	200–400/°C	400–900/°C	
pH 3						
Silica	92	↓	5	2	2	9
Silica–BSA	76/321/515	↓, ↑	4	5	4	13
pH 4.6						
Silica	86	↓	5	2	2	9
Silica–BSA	75/313/527	↓, ↑	3	7	5	15
pH 7.6						
Silica	89	↓	5	1	2	8
Silica–BSA	78/300/490	↓, ↑	4	5	3	12
pH 9						
Silica	87	↓	5	4	–	9
Silica–BSA	87/308/457	↓, ↑	5	5	3	13

system stability. In turn, low transmission and high backscatter level are characteristic of the high stability suspension. By analysing the distances between the curves, it is possible to determine the dynamics of the processes occurring in the sample. A large distance between the curves shows a low suspension stability and thus the high-speed particle migration as well as rapid sedimentation. In contrast, coverage of the individual curves demonstrates a high system stability and a much lower rate of particle sedimentation. The silica suspension stability was also evaluated based on the TSI (Turbiscan Stability Index) values (Table 2). This index is the average of processes occurring in the studied systems. The smaller the TSI value, the more stable the suspension is.

The silica suspension in the absence of albumin has a relatively low stability at pH 3 and 4.6 (the TSI values are 35.68 and 31.81, respectively). In these two cases, a low system stability is related to the zero adsorbent surface charge and the silica electrokinetic potential close to 0. An equal number of SiO_2^+ and SiO^- groups on the solid surface makes particles neutral to each other. Additionally, the similarity of concentrations of positively and negatively charged groups in the slipping plane is equivalent to the absence of electrostatic repulsion between the particles. The above phenomena allow the formation of solid aggregates of considerable sizes.

Table 2 TSI values for the silica suspension in the absence and presence of BSA (100 ppm) calculated using Eq. 2

System	TSI			
	pH 3	pH 4.6	pH 7.6	pH 9
Silica	35.68	31.81	3.77	3.03
Silica–BSA	1.05	43.06	1.54	1.95

At pH 7.6 and 9, the silica suspension without albumin has a high stability (TSI = 3.77 and 3.03, respectively). Under these conditions, the electrostatic system stabilization occurs, which is provided by the negative zeta potential values (−32 and −38 mV). Each negatively charged particle is surrounded by a diffusion layer of positive ions from the supporting electrolyte (Na^+), which prevents particle collision and aggregate formation.

The BSA addition affects the silica suspension stability in a different way, depending on the solution pH value. The biggest change in the system stability as a result of the albumin adsorption was observed at pH 3 (TSI value changed from 35.68 to 1.05). Under these conditions, strong system stabilization occurs, which is evidenced by the overlapping of the curves in the graphs showing transmission and backscatter of light passing through the sample during the measurement (Fig. 7a). For comparison, the mutual distance of the curves obtained in the albumin absence is clear (Fig. 7b). Based on the results of zeta potential measurements, it was found that during BSA adsorption, a whole solid surface is coated with the albumin macromolecules and then the solid surface properties are similar to those of the albumin. At pH 3, the BSA macromolecules are positively charged and thus electrosteric system stabilization is most likely under these conditions. It arises from the mutual repulsion of adsorption films formed on the silica surface as well as the mutual repulsion of positive charges of the BSA macromolecules. In this situation, solid aggregate formation is practically impossible. Strong stabilization by the BSA adsorption was also observed at pH 7.6 and 9 (TSI = 1.54 and 1.95, respectively). Under these conditions, the adsorption layers of negative macromolecules are formed on the silica surface and as a result, the particles also repel electrosterically.

At pH 4.6, the presence of albumin reduces the silica suspension stability (TSI = 43.06). In this case, the BSA

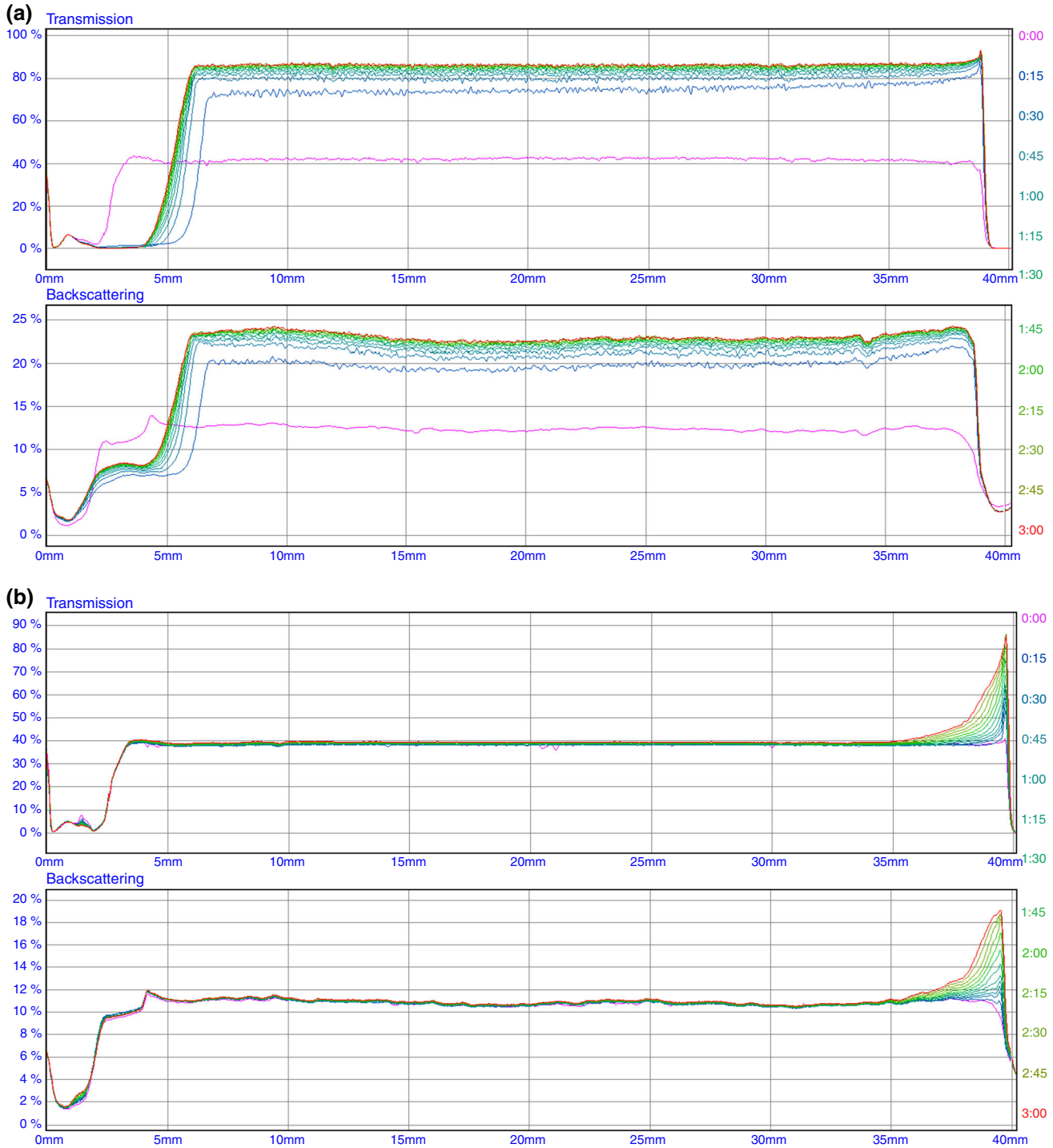

Fig. 7 Transmission and backscatter curves for the systems: **a** silica, **b** silica-BSA at pH 3

macromolecules adsorbed on the solid surface have a net charge close to zero, which is dictated by their pI point. Thus, there are no electrostatic repulsion forces in the system that hinder the particle contact.

Acknowledgements The research leading to these results has received funding from the People Programme (Marie Curie Actions) of the European Union's Seventh Framework Programme FP7/2007-2013/under REA grant agreement no. PIRSES-GA-2013-612484.

References

1. Silva-Bermudez P, Rodil SE. An overview of protein adsorption on metal oxide coatings for biomedical implants. Surf Coat Technol. 2013;233:147–58.
2. Fragala ME, Satriano C. Selective protein adsorption on ZnO thin films for biofunctional nano-platforms. J Nanosci Nanotechnol. 2010;10(9):5889–93.
3. Silva-Bermudez P, Rodil SE, Muhl S. Albumin adsorption on oxide thin films studied by spectroscopic ellipsometry. Appl Surf Sci. 2011;258(5):1711–8.
4. Adamczyk Z, Barbasz J, Ciesla M. Mechnisms of fibrynogen adsorption at solid substrates. Langmuir. 2011;27(11):6868–78.
5. Payet V, Dini T, Brunner S, Galtayries A, Frateur I, Marcus P. Pre-treatment of titanium surfaces by fibronectin: in situ adsorption and effect of concentration. Surf Interface Anal. 2010;42(6–7):457–61.
6. Johnson D. Removing beerstone. Modern Brewery Age. Birko Corporation R&D;1998.
7. Moreno-Arribas MV, Polo MC. Wine chemistry and biochemistry. Berlin: Springer; 2009.
8. Rashed MN. Adsorption technique for removal of organic pollutants from water and wastewater. Organic pollutants—monitoring, risk and treatment. doi:10.5772/54048.
9. Norde W, Tan W, Koopal L. Protein adsorption at solid surfaces and protein complexation with humicacids. In: 5th international sympsium ISMOM 2008, 24-28.11. Pucon, Chile.
10. Klinger A, Steinberg D, Kohavi D, Sela N. Mechnism of adsorption of human albumin to titanium in vitro. J Biomed Mater Res. 1997;36(3):387–92.
11. Rezwan K, Meier LP, Gauckler LJ. Lysozyme and bovine serum albumin adsorption on uncoated silica and AlOOH-coated silica particles: the influence of positively and negatively charged oxide surface coatings. Biomater. 2005;26:4351–7.
12. Han J, Silcock P, McQuillan AJ, Bremer P. Bovine serum albumin adsorption on N-methyl-D-glucamine modified colloidal silica. Colloids Surf A. 2009;349:207–13.
13. Kopac T, Bozgeyik K, Yener J. Effect of pH and temperature on the adsorption of bovine serum albumin onto titanium dioxide. Colloids Surf A. 2008;322:19–28.
14. Nosal-Wiercińska A. The influence of water activity on double layer parameters on the interface mercury/chlorates (VII) in the presence of cysteine. Croat Chem Acta. 2013;86(2):159–64.
15. Nosal-Wiercińska A. Intermolecular interactions in systems containing Bi(III)—ClO_4^-—H_2O—selected amino acids in the aspect of catalysis of Bi(III) electroreduction. Electroanal. 2014;26(5):1013–23.
16. Lundqvist M, Sethson I, Jonsson BH. Protein adsorption onto silica nanoparticles: conformational changes and the particles' curvature and the protein stability. Langmuir. 2004;20(24):10639–47.
17. Larsericsdotter H, Oscarsson S, Buijs J. Structure, stability and orientation of BSA adsorbed to silica. J Colloid Interface Sci. 2005;289(1):26–35.
18. Wells MA, Abid A, Kennedy IM, Barakat AI. Serum proteins prevent aggregation of Fe_2O_3 and ZnO nanoparticles. Nanotox. 2011. doi:10.3109/17435390.2011.623131.
19. Allouni ZE, Cimpan MR, Hol PJ, Skodvin T, Gjerdet NR. Agglomeration and sedimentation of TiO_2 nanoparticles in cell culture medium. Colloids Surf B. 2009;68:83–7.
20. Vamann CI, Hol PJ, Allouni ZE, Elsayed S, Gjerdet NR. Formation of potential titanium antigens based on protein binding to titanium dioxide nanoparticles. Int J Nanomed. 2008;3:69–74.
21. Flynn RM, Yang X, Hofmann T, Von der Kammer F. Bovine serum albumin adsorption to iron-oxide coated sands can change microsphere deposition mechanisms. Environ Sci Technol. 2012;46:2583–91.
22. Gładysz-Płaska A, Majdan M, Sternik D, Pikus S, Zięba E. Sorptive and thermal properties of red clay in relation to Cr(VI). J Therm Ana Calorim. 2010;101(2):775–8.
23. Sternik D, Staszczuk P, Majdan M, Gładysz-Płaska A, Dąbrowska E, Bigda K. Studies of physico-chemical properties of mixed adsorbent in the zeolite/SiO_2 system. J Therm Ana Calorim. 2006;86(1):69–75.
24. Wiśniewska M. Temperature effect on adsorption properties of silica-polyacrylic acid interface. J Them Ana Calorim. 2010;101(2):753–60.
25. Wiśniewska M. Studies of temperature influence on adsorption behavior of nonionic polymers at the zirconia-solution interface. J Therm Ana Calorim. 2010;101(2):743–51.
26. Wiśniewska M, Chibowski S, Urban T, Sternik D. Investigation of the alumina properties with adsorbed polyvinyl alcohol. J Therm Ana Calorim. 2011;103(1):329–37.
27. Yang Y, Ma H. Western blotting and ELISA techniques. Researcher. 2009;1(2):67–86.
28. Gurav JL, Jung I, Park H, Kang ES, Nadargi DY. Silica aerogel: synthesis and applications. J Nanomat. 2010. doi:10.1155/2010/409310.
29. Dolley TP. Silica. US Geological survey and minerals yearbook; 2004.
30. Reed RG, Putnam FW, Peters T. Sequence of residues 400–403 of bovine serum albumin. Biochem J. 1980;191:867–8.
31. Dawson RMC. Data for biochemical research. 3rd ed. Oxford: Clarendon Press; 1986.
32. Abramson HAMLS, Gorin MH. Electrophoresis of proteins. New York: Hafner Publishing Company; 1942.
33. Rezwan K, Meier LP, Rezwan M, Voros J, Textor M, Gauckler LJ. Bovine serum albumin adsorption onto colloidal Al_2O_3 particles: new model based on zeta potential and UV–Vis measurements. Langmuir. 2004;20:10055–61.
34. Norde W, MacRitchie F, Nowicka G, Lyklema J. Protein adsorption at solid-liquid interfaces: reversibility and conformation aspects. J Coll Sci. 1986;112:447–56.
35. Putnam FW. The plasma proteins: structure, function and genetic control. 2nd ed. New York: Academic Press; 1975.
36. Bos OJM, Labro JF, Fischer MJ, Wilting J, Janssen LH. The molecular mechanisms of the large peptic and a large tryptic fragment of albumin. J Biol Chem. 1989;264:953–9.
37. Janusz W. Electrical double layer at metal oxide-electrolyte interface in 'interfacial forces and fields theory and applications'. New York: M. Dekker; 1999.
38. Paulik F. Special trends in thermal analysis. New York: Wiley; 1995.
39. Hartvig RA, Van de Weert M, Ostergaard J, Jorgensen L, Jensen H. Protein adsorption at charged surfaces: the role of electrostatic interactions and interfacial charge regulation. Langmuir. 2011;27:2634–43.
40. Szewczuk-Karpisz K, Wiśniewska M. Investigation of removal possibilities of chromium(III) oxide from water solution in the presence of albumins. Int J Environ Sci Technol. 2014. doi:10.1007/s13762-014-0712-y.

41. Szewczuk-Karpisz K, Wiśniewska M. Adsorption properties of the albumin—chromium(III) oxide system—effect of solution pH and ionic strength. Soft Mater. 2014;12(3):268–76.
42. Foster JF. Albumin structure, function and uses. Oxford: Pergamon; 1977.
43. Zaharescu M, Jitianu A, Braileanu A, Madarasz J, Novalk C, Pokol G. Composition and thermal stability of SiO_2-based hybrid materials TEOS-MTEOS system. J Therm Anal Cal. 2003;71:421–8.
44. Swain SK, Sarkar D. Study of BSA protein adsorption/release on hydroxyapatite nanoparticles. App Surf Sci. 2013;286:99–103.
45. Han Y, Li S, Wang X, Jia L, He J. Preparation of hydroxyapatite rod-like crystals by protein precursor metod. Mat Res Bull. 2007;42:1169–77.
46. Giacomelli CE, Norde W. The adsorption-desorption cycle. Reversibility of the BSA-silica system. J Colloid Interface Sci. 2001;233:234–40.
47. Norde W, Giacomelli CE. BSA structural changes during homomolecular exchange between the adsorbed and the dissolved states. J Biotech. 2000;79:259–68.
48. Dasgupta S, Bandyopadhyay A, Bose S. Zn and Mg doped hydroxyapatite nanoparticles for controlled release of protein. Langmuir. 2010;26:4958–64.